

Synthesis, Characterization, and Induction of Stable Anisotropy in Liquid Crystalline Photo-addressable PPI Dendrimers

Rafael Alcalá,[†] Raquel Giménez,[‡] Luis Oriol,[‡] Milagros Piñol,^{*,‡} José Luis Serrano,[‡] Belén Villacampa,^{*,†} and Ana I. Viñuales[‡]

Departamento de Química Orgánica and Departamento de Física de la Materia Condensada, Facultad de Ciencias-ICMA, Universidad de Zaragoza-CSIC, 50009 Zaragoza, Spain

Received July 25, 2006. Revised Manuscript Received November 10, 2006

A series of liquid crystalline azobenzene codendrimers with light-driven properties has been prepared by chemical modification of the third generation of an amine-terminated poly(propylene imine) (PPI) dendrimer. These photoactive dendrimers were obtained by grafting the photochromic 4-cyanoazobenzene and/or liquid crystalline 4-cyanobiphenyl units onto the periphery of PPI. The synthesized dendrimers include different percentages of each functional unit randomly distributed in the dendritic shell. The chemical structures of the dendrimers were characterized by several techniques to determine their composition. In particular, MALDI-TOF analysis provided detailed information about the chemical composition of the dendrimers. The photo-induced orientation of azobenzene groups in thin films of these dendrimers was studied. Illumination with either blue (488 nm) or UV (350 nm) linearly polarized light at room temperature gave rise to a stable dichroism and moderate birefringence values when 80% (molar ratio) of the units are azobenzene. In addition, pre-irradiation of the films with unpolarized UV light gave rise to higher birefringence values.

Introduction

Since dendritic structures were identified as a new class of polymers, scientists have devoted a great deal of effort to the investigation of these systems with the aim of finding novel and improved properties resulting from their unusual and well-defined architecture.^{1–3} In fact, dendritic molecules possess a perfectly controlled structure consisting of an internal core surrounded by a branched shell that carries a defined number of peripheral groups. The appropriate design of the chemical structure enables the incorporation in these nanometer-sized molecules of a defined number of specific functional groups at specific locations, a feature that endows the dendrimers with their versatile nature. Furthermore, the dendritic scaffold can be chemically modified to incorporate an increasing number of active moieties with specific properties. Given the availability of numerous surface-modified dendrimers, the field has evolved from the establishment of synthetic approaches and the synthesis of novel dendrimers to the characterization of their properties and potential applications in such diverse fields as medicine, biology, chemistry, materials science, and engineering.^{4–11}

In particular, the design of functional dendrimers by peripheral modification with photo- or electroactive moieties can result in interesting specific functions because their spatially uniform arrangement can provide a highly dense distribution of disentangled functional moieties, a situation that makes unique photochemical and photophysical properties easy to tune and manipulate.^{12,13}

The generation of anisotropy in films of organic materials is a fundamental aspect of research in materials science and can improve the properties of devices for many optical technologies. Among photoactive moieties, azobenzene and its analogues are unique photoresponsive systems that are able to change their optical properties under light irradiation and undergo a photo-induced orientation under polarized light. Upon exposure to light of different wavelengths, the azobenzene undergoes a clean, fast and reversible photo-induced *E/Z* isomerization associated with significant changes in the absorption spectra and the structural parameters of the moiety. This behavior is the basis for numerous technological applications, many of which are based on optically anisotropic polymer films due to the fact that photo-induced orientation of azobenzene groups under polarized light is a

* Address correspondence to either author. E-mail: mpinol@unizar.es (M.P.) or bvillaca@unizar.es (B.V.).

[†] Departamento de Física de la Materia Condensada.

[‡] Departamento de Química Orgánica.

- (1) Newkome, G. R.; Moorefield, C. N.; Vogtle, F. *Dendritic Molecules: Concepts, Synthesis, Perspectives*; VCH: Weinheim, 1996.
- (2) Bosman, A. W.; Janssen, H. M.; Meijer, E. W. *Chem. Rev.* **1999**, *99*, 1665–1688.
- (3) Tomalia, D. A. *Prog. Polym. Sci.* **2005**, *30*, 294–324.
- (4) Inoue, K. *Prog. Polym. Sci.* **2000**, *25*, 453–571.
- (5) Boas, U.; Heegaard, P. M. H. *Chem. Soc. Rev.* **2004**, *33*, 43–63.
- (6) Hecht, S.; Frechet, J. M. J. *Angew. Chem., Int. Ed.* **2001**, *40*, 74–91.
- (7) Aulenta, F.; Hayes, W.; Rannard, S. *Eur. Polym. J.* **2003**, *39*, 1741–1771.

- (8) Momotake, A.; Arai, T. *Polymer* **2004**, *45*, 5369–5390.
- (9) Balzani, V.; Ceroni, P.; Maestri, M.; Saudan, C.; Vicinelli, V. In *Dendrimers V: Functional and Hyperbranched Building Blocks, Photophysical Properties, Applications in Materials and Life Sciences*; Springer: London, 2003; Vol. 228, pp 159–191.
- (10) van de Coevering, R.; Gebbink, R.; van Koten, G. *Prog. Polym. Sci.* **2005**, *30*, 474–490.
- (11) Luo, J. D.; Ma, H.; Jen, A. K. Y. *C. R. Chim.* **2003**, *6*, 895–902.
- (12) Hahn, U.; Gorka, M.; Vogtle, F.; Vicinelli, V.; Ceroni, P.; Maestri, M.; Balzani, V. *Angew. Chem., Int. Ed.* **2002**, *41*, 3595–3598.
- (13) Vogtle, F.; Gorka, M.; Hesse, R.; Ceroni, P.; Maestri, M.; Balzani, V. *Photochem. Photobiol. Sci.* **2002**, *1*, 45–51.

well-known process.^{14–26} In most of the studies reported to date, anisotropy has been induced by illumination with linearly polarized light (488 nm) from an Ar⁺ laser. Under this illumination a preferential orientation of the *E* molecules, in which the axis is perpendicular to the polarization direction of the exciting light, can be achieved. High and stable optical anisotropy, examined by dichroism and birefringence measurements, has been obtained in films of liquid crystalline copolymers (LCP) with azobenzene units in the side chain in which the cooperative motions among their constitutional units have played an important role.^{27–33}

Dendrimers with photo-responsive azobenzene fragments represent an interesting subclass of light-sensitive polymers.^{8,26,34–36} On the basis of their photo-switchable properties, dendrimers with azobenzene fragments localized at the core, either through the branches or appended to their surface, have been investigated for a variety of purposes including applications as photo-switchable hosts,³⁷ light-harvesting systems,³⁸ and holographic recording.³⁹ Most of the reports found in the literature describe the behavior of dendrimers in solution, and in general, the activity of the azobenzene is not perturbed

by its incorporation into the dendrimer structure. Papers have also been published that describe how the macroscopic behavior of vesicles or Langmuir–Blodgett monolayers formed by azobenzene dendrimers can be controlled by light.^{40,41} However, very few publications are concerned with the peculiarities of photochemical behavior in films, particularly in relation to polarized light.^{26,42,43} In one example, the photo-orientation of a first-generation carbosilane liquid crystalline dendrimer with propyloxyazobenzene units grafted onto the periphery was studied.⁴³ It was shown that irradiation of an amorphous film with polarized light (488 nm) induces a linear dichroism ($D = 0.16$) that tends to decrease to zero several hours after the irradiation is ceased. Besides, photo-orientation of the azo groups was almost absent upon irradiation with polarized UV light. Contrasting behavior was seen on studying different generations ($n = 1, 3, 5$) of carbosilane dendrimers with ethoxyazobenzene substituents.⁴² A linear dichroism was generated on UV irradiation that was unstable regardless of generation, but 488 nm light did not produce any orientational effect. The possible use of azobenzene-functionalized poly(propylene imine) (PPI) dendrimers in holographic data storage has also been explored, and holographic gratings with diffraction efficiencies up to 20% and good thermal stabilities were recorded in first and second generation dendrimers.³⁹

The purpose of the work described here was the synthesis of a series of PPI dendrimers with liquid crystalline and photochromic properties with the aim of investigating the capability of light-addressable units to achieve a stable macroscopic alignment at room temperature (RT). We describe the peripheral modification of a third generation PPI dendrimer with the 4-cyanobiphenyl mesogenic (CNB) unit and the 4-cyanoazobenzene photochromic unit (AZO) (see Figure 1). Three codendrimers containing the two functional units randomly distributed at the periphery of the PPI, which contain CNB/AZO molar ratios of 90:10, 80:20, and 20:80, and the two corresponding homodendrimers, PPI-CNB and PPI-AZO, were investigated. Our initial aim was to study the behavior of the PPI homodendrimer PPI-AZO. However, given the solubility problems described in the text, the azobenzene content was reduced to 80% molar ratio by the incorporation 4-cyanobiphenyl, a liquid crystalline unit that can work cooperatively during photo-induction processes. In addition, codendrimers with low percentages of azobenzene (20 and 10%) in the dendritic scaffold were prepared to elucidate the possibility of achieving an adequate response on reducing the absorption problems associated with high azobenzene contents. Therefore, we examined the photo-orientation processes of the azo-containing dendrimers by measuring the linear dichroism and birefringence on dendrimer films after illumination with 488 nm polarized light. Photo-induced anisotropy measurements under polarized UV

- (14) Eich, M.; Wendorff, J. J. *Opt. Soc. Am. B* **1990**, *7*, 1428–1436.
- (15) Anderle, K.; Birenheide, R.; Werner, M. J. A.; Wendorff, J. H. *Liq. Cryst.* **1991**, *9*, 691–699.
- (16) Rochon, P.; Gosselin, J.; Natansohn, A.; Xie, S. *Appl. Phys. Lett.* **1992**, *60*, 4–5.
- (17) Natansohn, A.; Rochon, P.; Gosselin, J.; Xie, S. *Macromolecules* **1992**, *25*, 2268–2273.
- (18) Natansohn, A.; Rochon, P. *Chem. Rev.* **2002**, *102*, 4139–4175.
- (19) Fischer, T.; Lasker, L.; Stumpe, J.; Kostromin, S. G. *J. Photochem. Photobiol., A* **1994**, *80*, 453–459.
- (20) Lasker, L.; Fischer, T.; Stumpe, J.; Kostromin, S.; Ivanov, S.; Shibaev, V.; Ruhmann, R. *Mol. Cryst. Liq. Cryst. Sci. Technol., Sect. A* **1994**, *252*, 293–302.
- (21) Lasker, L.; Fischer, T.; Stumpe, J.; Kostromin, S.; Ivanov, S.; Shibaev, V.; Ruhmann, R. *Mol. Cryst. Liq. Cryst. Sci. Technol., Sect. A* **1994**, *246*, 347–350.
- (22) Lasker, L.; Stumpe, J.; Fischer, T.; Rutloh, M.; Kostromin, S.; Ruhmann, R. *Mol. Cryst. Liq. Cryst. Sci. Technol., Sect. A* **1995**, *261*, 371–381.
- (23) Holme, N. C. R.; Ramanujam, P. S.; Hvilsted, S. *Appl. Opt.* **1996**, *35*, 4622–4627.
- (24) Wu, Y. L.; Demachi, Y.; Tsutsumi, O.; Kanazawa, A.; Shiono, T.; Ikeda, T. *Macromolecules* **1998**, *31*, 349–354.
- (25) Cimrova, V.; Neher, D.; Kostromin, S.; Bieringer, T. *Macromolecules* **1999**, *32*, 8496–8503.
- (26) Shibaev, V.; Bobrovsky, A.; Boiko, N. *Prog. Polym. Sci.* **2003**, *28*, 729–836.
- (27) Ikeda, T.; Miyamoto, T.; Kurihara, S.; Tsukada, M.; Tazuke, S. *Mol. Cryst. Liq. Cryst.* **1990**, *182*, 373–385.
- (28) Lee, H. K.; Kanazawa, A.; Shiono, T.; Ikeda, T.; Fujisawa, T.; Aizawa, M.; Lee, B. *Chem. Mater.* **1998**, *10*, 1402–1407.
- (29) Fischer, T.; Lasker, L.; Rutloh, M.; Czaplá, S.; Stumpe, J. *Mol. Cryst. Liq. Cryst. Sci. Technol., Sect. A* **1997**, *299*, 293–299.
- (30) Rutloh, M.; Stumpe, J.; Stachanov, L.; Kostromin, S.; Shibaev, V. *Mol. Cryst. Liq. Cryst.* **2000**, *352*, 583–591.
- (31) Meier, J. G.; Ruhmann, R.; Stumpe, J. *Macromolecules* **2000**, *33*, 843–850.
- (32) Rosenhauer, R.; Fischer, T.; Czaplá, S.; Stumpe, J.; Vinuales, A.; Pinol, M.; Serrano, J. L. *Mol. Cryst. Liq. Cryst.* **2001**, *364*, 295–304.
- (33) Rosenhauer, R.; Fischer, T.; Stumpe, J.; Gimenez, R.; Pinol, M.; Serrano, J. L.; Vinuales, A.; Broer, D. *Macromolecules* **2005**, *38*, 2213–2222.
- (34) Momotake, A.; Arai, T. *J. Photochem. Photobiol., C* **2004**, *5*, 1–25.
- (35) Villavicencio, O.; McGrath, D. V. In *Advances in Dendritic Macromolecules*; Newkome, G. R., Ed.; Elsevier Science: Oxford, 2002; Vol. 5, pp 1–44.
- (36) Vogtle, F.; Gestermann, S.; Hesse, R.; Schwierz, H.; Windisch, B. *Prog. Polym. Sci.* **2000**, *25*, 987–1041.
- (37) Archut, A.; Azzellini, G. C.; Balzani, V.; De Cola, L.; Vogtle, F. *J. Am. Chem. Soc.* **1998**, *120*, 12187–12191.
- (38) Jiang, D. L.; Aida, T. *Nature* **1997**, *388*, 454–456.
- (39) Archut, A.; Vogtle, F.; De Cola, L.; Azzellini, G. C.; Balzani, V.; Ramanujam, P. S.; Berg, R. H. *Chem. Eur. J.* **1998**, *4*, 699–706.

- (40) Dol, G. C.; Tsuda, K.; Weener, J. W.; Bartels, M. J.; Asavei, T.; Gensch, T.; Hofkens, J.; Latterini, L.; Schenning, A.; Meijer, B. W.; De Schryver, F. C. *Angew. Chem., Int. Ed.* **2001**, *40*, 1710–1714.
- (41) Weener, J. W.; Meijer, E. W. *Adv. Mater.* **2000**, *12*, 741–746.
- (42) Bobrovsky, A.; Ponomarenko, S.; Boiko, N.; Shibaev, V.; Rebrov, E.; Muzafarov, A.; Stumpe, J. *Macromol. Chem. Phys.* **2002**, *203*, 1539–1546.
- (43) Bobrovsky, A. Y.; Pakhomov, A. A.; Zhu, X. M.; Boiko, N. I.; Shibaev, V. P.; Stumpe, J. *J. Phys. Chem. B* **2002**, *106*, 540–546.

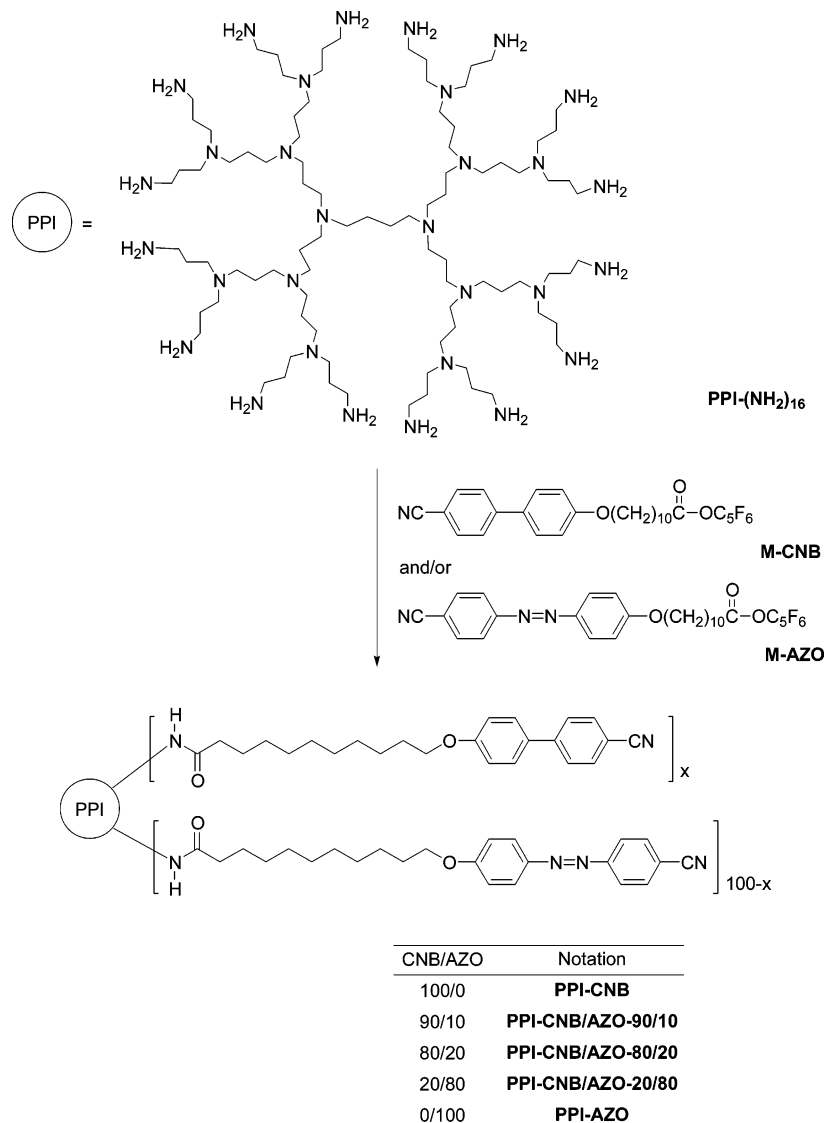


Figure 1. Schematic representation of functionalized dendrimers obtained by chemical modification of the third generation poly(propylene imine) dendrimer with 16 primary amino groups in the periphery [PPI-(NH₂)₁₆]. The reaction was carried out in dichloromethane under reflux for 4 days.

light were performed, and the influence of UV pre-irradiation on the photo-induced processes was also investigated.

Experimental Section

Synthesis of Materials. Pentafluorophenyl 11-[4'-cyano-4-biphenyloxy]undecanoate [M-CNB] was synthesized as reported.⁴⁴ Pentafluorophenyl 11-[4'-cyanophenylazophenyl]undecanoate [M-AZO] was prepared from 4-cyano-4'-hydroxyazobenzene, which was obtained by diazotization of 4-aminobenzonitrile with sodium nitrite and coupling with phenol, using the same procedure.

General Procedure for Synthesis of the Dendrimers and Codendrimers. All the dendrimers were prepared following the general procedure detailed for PPI-CNB but with some modifications that are described in each particular case.

Synthesis and Characterization of PPI-CNB. Commercial PPI-(NH₂)₁₆ (140 mg, 8.0 × 10⁻² mmol) in CH₂Cl₂ (2 mL) was slowly added to a solution M-CNB (800 mg, 1.5 mmol) in CH₂Cl₂ (30 mL). After completion of the addition, the reaction mixture was heated under reflux for 4 days. The solution was allowed to cool

down to room temperature and was diluted with a 1:1 mixture of CH₂Cl₂/methanol (15 mL). After washing with saturated aqueous Na₂CO₃ (2 × 40 mL), the organic phase was dried over MgSO₄ and filtered, and the solvent evaporated under reduced pressure. The crude product was purified twice by dissolving in the minimum volume of CH₂Cl₂ and precipitating with hexane to yield a white powder (72% yield). ¹H NMR (400 MHz, CDCl₃, δ): 7.64 (d, *J* = 8.1 Hz, 32H), 7.58 (d, *J* = 8.4 Hz, 32H), 7.47 (d, *J* = 8.4 Hz, 32H), 7.09 (br t, 16H), 6.93 (d, *J* = 8.4 Hz), 3.94 (t, *J* = 6.4 Hz), 3.24–3.22 (m), 2.35 (m), 2.18–2.13 (m), 1.77–1.72 (m), 1.52–1.26 (m). ¹³C NMR (100 MHz, CDCl₃, δ): 173.7, 159.8, 157.5, 145.2, 132.6, 131.3, 128.3, 128.2, 127.0, 119.0, 115.1, 110.1, 68.1, 52.2, 51.4, 38.1, 37.7, 36.6, 29.5, 29.4, 29.2, 29.1, 27.1, 26.1, 25.9, 25.8. IR (KBr, cm⁻¹): 3294, 3088 (NH), 2921, 2850 (CH₂), 2226 (C≡N), 1640 (C=O), 1602, 1549, 1494 (C–Car), 1288, 1252, 1217 (C–O). Anal. Found (calcd): C 75.14% (75.89), H 8.64% (8.64), N 9.01% (8.62). GPC (CH₂Cl₂ + 1% Et₃N): polydispersity index = 1.08.

Synthesis PPI-CNB/AZO-90/10. The synthesis was performed using a solution of PPI-(NH₂)₁₆ (108 mg, 6.0 × 10⁻² mmol) in CH₂Cl₂ (2 mL) and a 90:10 molar ratio of M-CNB (550 mg, 1.01 mmol) and M-AZO (6.42 mg, 0.11 mmol) in CH₂Cl₂ (25 mL). After

(44) Baars, M.; Sontjens, S. H. M.; Fischer, H. M.; Peerlings, H. W. I.; Meijer, E. W. *Chem. Eur. J.* **1998**, *4*, 2456–2466.

purification a pale orange solid was obtained (62% yield). ^1H NMR (400 MHz, CDCl_3 , δ): 7.90 (d, $J = 8.5$ Hz), 7.76 (d, $J = 8.4$ Hz), 7.66 (d, $J = 8.5$ Hz), 7.60 (d, $J = 8.8$ Hz), 7.49 (d, $J = 8.5$ Hz), 7.40–7.10 (br t), 6.98–6.93 (m), 4.00, 3.96 (m), 3.29–3.20 (m), 2.45–2.26 (m), 2.18 (t, $J = 7.6$ Hz), 1.81–1.60 (m), 1.58–1.18 (m). ^{13}C NMR (100 MHz, CDCl_3 , δ): 173.7, 159.7, 145.1, 133.1, 132.5, 131.2, 128.3, 127.0, 125.4, 123.0, 119.0, 115.1, 110.1, 68.1, 52.1, 51.4, 37.8, 36.7, 32.2, 29.6, 29.5, 29.4, 27.2, 26.4, 26.1, 25.9, 23.4. IR (KBr, cm^{-1}): 3294, 3073 (NH), 2920, 2850 (CH_2), 2226 ($\text{C}\equiv\text{N}$), 1639 ($\text{C}=\text{O}$), 1603, 1551, 1495 (C–Car), 1290, 1252, 1219 (C–O). Anal. Found (calcd): C 76.20% (75.43), H 7.81% (8.60), N 9.61% (9.17). GPC ($\text{CH}_2\text{Cl}_2 + 1\%$ Et_3N): polydispersity index = 1.15.

Synthesis of PPI-CNB/AZO-80/20. The synthesis was carried out following the same procedure described for PPI-CNB/AZO-90/10 but using M-CNB/M-AZO in a 4:1 molar ratio. After purification a pale orange solid was obtained (83% yield). ^1H NMR (400 MHz, CDCl_3 , δ): 7.88 (d, $J = 8.1$ Hz), 7.74 (d, $J = 8.2$ Hz), 7.64 (d, $J = 8.3$ Hz), 7.58 (d, $J = 7.9$ Hz), 7.47 (d, $J = 8.9$ Hz), 7.10 (br), 6.95 (d, $J = 6.5$ Hz), 6.91 (d, $J = 8.6$ Hz), 3.96 (t, $J = 7.4$ Hz), 3.93 (t, $J = 6.2$ Hz), 3.23–3.21 (m), 2.42–2.35 (m), 2.15 (t, $J = 7.6$ Hz), 1.79–1.58 (m), 1.46–1.26 (m). ^{13}C NMR (100 MHz, CDCl_3 , δ): 173.8, 162.6, 159.7, 146.7, 145.1, 133.1, 132.5, 131.2, 128.3, 127.0, 125.4, 123.0, 119.1, 118.6, 115.0, 114.8, 110.0, 68.4, 68.1, 52.0, 51.2, 37.7, 36.6, 29.4, 27.0, 25.9. IR (KBr, cm^{-1}): 3296, 3072 (NH), 2921, 2850 (CH_2), 2225 ($\text{C}\equiv\text{N}$), 1640 ($\text{C}=\text{O}$), 1603, 1549, 1494 (C–Car), 1289, 1252 (C–O). Anal. Found (calcd): C 75.04% (74.98), H 7.38% (8.55), N 9.28% (9.71). GPC ($\text{CH}_2\text{Cl}_2 + 1\%$ Et_3N): polydispersity index = 1.13.

Synthesis of PPI-CNB/AZO-20/80. The reaction was carried out as described for PPI-CNB/AZO-90/10, using M-CNB/M-AZO in a 1:4 molar ratio. In this case the product precipitated during the course of the reaction and was isolated by filtration and washed several times with CH_2Cl_2 and methanol to render an orange solid (60% yield). ^1H NMR (400 MHz, tetrachloroethane- d_2 , 65 °C, δ): 7.90 (d, $J = 8.0$ Hz), 7.75 (d, $J = 7.5$ Hz), 7.66–7.57 (m), 7.53–7.45 (m), 7.04–6.90 (m), 6.77–6.65 (m), 4.10–3.80 (m), 3.32–3.05 (m), 2.70–2.25 (m), 2.20–1.95 (m), 1.88–0.90 (m). ^{13}C NMR (100 MHz, tetrachloroethane- d_2 , 65 °C, δ): 170.5, 158.9, 156.7, 151.0, 143.0, 141.3, 135.7, 129.2, 128.7, 127.3, 124.4, 123.1, 121.6, 119.2, 115.2, 114.8, 111.5, 111.2, 109.2, 106.2, 64.8, 64.5, 47.1, 32.9, 32.6, 25.7, 25.6, 25.3, 22.1, 21.9, 20.0. IR (KBr, cm^{-1}): 3300, 3089 (NH), 2921, 2848 (CH_2), 2227 ($\text{C}\equiv\text{N}$), 1641 ($\text{C}=\text{O}$), 1601, 1579, 1549, 1495 (C–Car), 1292, 1249 (C–O). Anal. Found (calcd): C 71.50% (72.40), H 7.89% (8.25), N 12.73% (12.29). GPC ($\text{CH}_2\text{Cl}_2 + 1\%$ Et_3N): insoluble.

Synthesis of PPI-AZO. In this case, after addition of the monomer was complete, an orange solid precipitated during the course of the reaction. The suspension was stirred and heated under reflux for 4 days. The orange solid was isolated by filtration and washed with CH_2Cl_2 and methanol (91% yield). ^1H NMR (300 MHz, tetrachloroethane- d_2 , 65 °C, δ): 7.90 (d, $J = 8.8$ Hz, 64H), 7.74 (d, $J = 8.5$ Hz), 6.97 (d, $J = 8.7$ Hz), 6.75–6.60 (m), 4.12–3.85 (m), 3.30–3.10 (br), 2.75–2.30 (m), 2.18–1.98 (m), 1.90–1.00 (m). ^{13}C NMR (75 MHz, tetrachloroethane- d_2 , 65 °C, δ): 174.3, 162.5, 154.7, 150.8, 146.6, 139.8, 136.1, 132.9, 125.2, 122.8, 118.4, 114.8, 114.8, 112.8, 68.4, 50.7, 36.5, 36.2, 29.2, 29.1, 28.9, 25.7, 25.5, 21.3, 23.9. IR (KBr, cm^{-1}): 3286, 3075 (NH), 2920, 2848 (CH_2), 2227 ($\text{C}\equiv\text{N}$), 1641 ($\text{C}=\text{O}$), 1599, 1579, 1537, 1496 (C–Car), 1290, 1247 (C–O). Anal. Found (calcd): C 70.32% (71.59), H 7.80% (8.15), N 12.73% (13.80). GPC ($\text{CH}_2\text{Cl}_2 + 1\%$ Et_3N): insoluble.

Characterization Techniques. Elemental analysis was performed with a Perkin-Elmer 2400 series II microanalyzer. IR spectra

were measured on a NICOLET Avatar 380 or ATI-Matsson Genesis series FTIR spectrophotometer using KBr pellets. ^1H NMR and ^{13}C NMR spectra were recorded on a BRUKER ARX-300 spectrometer at 300 MHz for ^1H and at 75 MHz for ^{13}C . ^{19}F NMR spectra were recorded on a BRUKER AV-400 spectrometer at 282 MHz. Matrix-assisted laser desorption ionization–time-of-flight mass spectrometry (MALDI-TOF–TOF) was performed at the Sidi Service of the Universidad Autónoma (Madrid) on a 4700 Proteomic analyzer from Applied Biosystems. Dithranol or α -cyano-4-hydroxycinnamic acid was used as a matrix and, when required, sodium iodide as a cationic agent matrix. Dendrimers were dissolved in dichloromethane or dichloromethane/trifluoroacetic acid (TFA). Gel permeation chromatography (GPC) was carried out on a Waters liquid chromatography system equipped with 600E multisolvent delivery system and a 996 photodiode array detector, using a combination of two Ultrastaygel columns with pore size of 500 and 10^4 Å, calibrated using polystyrene standards. To reduce peak broadening and tailing in the chromatograms due to adsorption effects, CH_2Cl_2 with 1% triethylamine was used as the mobile phase at a flow rate of 0.8 mL/min.⁴⁵ Mesogenic behavior and transition temperatures were determined using an Olympus BH-2 polarizing microscope equipped with a Linkam THMS hot-stage central processor and a CS196 cooling system. Differential scanning calorimetry (DSC) was performed using a DSC 2910 from TA Instruments with samples sealed in aluminum pans and a scanning rate of 10 °C/min under a nitrogen atmosphere. Temperatures were read at the maximum of the transition peaks, and the glass transition temperature was read at the midpoint of the heat capacity increase. Thermogravimetric analysis (TGA) was performed using a TA Instruments STD 2960 simultaneous TGA-DTA at a rate of 10 °C/min under a nitrogen atmosphere. TGA data are given as the onset of the decomposition curve. In addition, the first derivative of the decomposition curve (DTGA) was read. Optical absorption spectra were recorded with an UV–vis spectrophotometer UV4-200 from ATI-Unicam.

Optical Measurements in Films. In order to study the photo-orientation properties, thin films were produced by casting solutions of the dendrimers onto clean fused quartz substrates. Dichloromethane was used as the solvent for PPI-CNB/AZO-80/20 and -90/10 codendrimers whereas PPI-AZO and PPI-CNB/AZO-20/80 were dissolved in cyclohexanone. The solubilities of the compounds with high azobenzene contents were quite poor even when hot solvent was used and the quality of the homodendrimer films was poor. Film thickness was measured using a DEKTAK 3ST contact profilometer. The thicknesses of the different samples ranged from 0.25 to 0.4 μm . Before performing any experiment, the films were heated to about 20 °C above the isotropization temperature, T_i , for 1 min and then rapidly quenched to room temperature (RT) by placing them on a metal plate to avoid any influence from the morphology induced during the preparation of the film and to erase any previously photo-induced effect. The homodendrimer films showed evidence of degradation on this pretreatment. Consequently, it was not possible to study the photo-orientation process of PPI-AZO under the required conditions.

A high-pressure Hg lamp in conjunction with a band-pass UV filter (transmission centered at 350 nm) was used as the UV light source. The measured light intensity was about 0.5 mW/cm² in the film.

Polarized optical absorption measurements were performed in a Cary 500 Scan UV–vis-NIR spectrophotometer. Linear (vertical/horizontal) polarization of the measuring beams was achieved using

(45) Bu, L. J.; Nonidez, W. K.; Mays, J. W.; Tan, N. B. *Macromolecules* **2000**, *33*, 4445–4452.

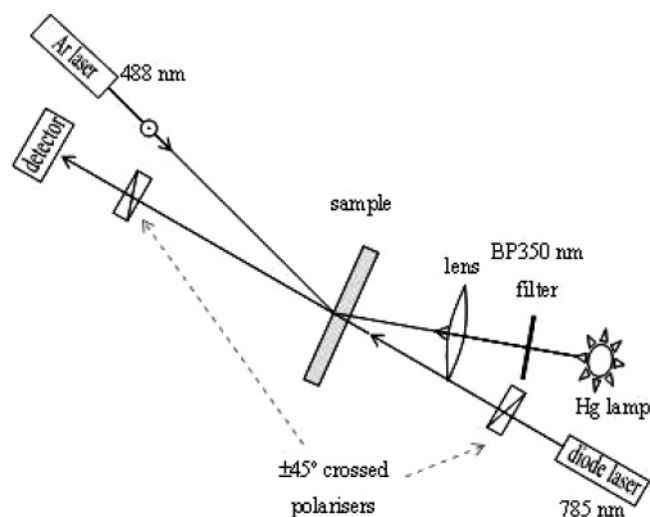


Figure 2. Experimental setup for birefringence measurements

a Glan–Thomson prism. The linear dichroism was calculated using

$$D = (A_{\parallel} - A_{\perp}) / (A_{\parallel} + A_{\perp}) \quad (1)$$

where A_{\parallel} and A_{\perp} are the optical absorbances measured with light horizontally and vertically polarized, respectively.

Photo-induced birefringence measurements were performed using the setup shown in Figure 2. The photo-orientation experiments were performed with vertically polarized light from an Ar⁺ laser at 488 nm (about 60 mW/cm²) or, alternatively, with the aforementioned Hg lamp and the band-pass filter plus a UV polarizer. The sample was placed between crossed polarizers with their polarization directions at $\pm 45^\circ$ with respect to the vertical axis. The photo-induced anisotropy was probed using light from a 785 nm diode laser transmitted through the polarizer–sample–polarizer system and measured with a Si detector. This light, with a power of about 1 W/cm², did not produce any changes in the optical anisotropy of the film within the experimental accuracy of our setup ($\Delta n \approx 10^{-3}$) after 1 h of irradiation. The transmitted intensity I is given by

$$I = I_0 \sin^2(\pi |\Delta n| d / \lambda) \quad (2)$$

where I_0 is the intensity transmitted with parallel polarizers when the film is in the initial isotropic state, d is the film thickness, Δn is the birefringence of the sample, and λ is the wavelength of the measuring light (785 nm).

Results and Discussion

Synthesis and Characterization of the Materials. Dendrimers were synthesized by grafting 4-cyanoazobenzene and 4-cyanobiphenyl units onto the periphery of the amine-terminated PPI core as outlined in Figure 1. The third generation PPI was selected to limit the solubility problems associated with higher generations, which would hinder the characterization and processability of the materials but still retain properties of polymeric materials like low crystallinity. The active units were incorporated through a decamethylene flexible spacer in order to decouple the molecular movements of the dendritic matrix and functional units. A shorter hexamethylene spacer was initially incorporated, but it gave rise to insoluble materials.

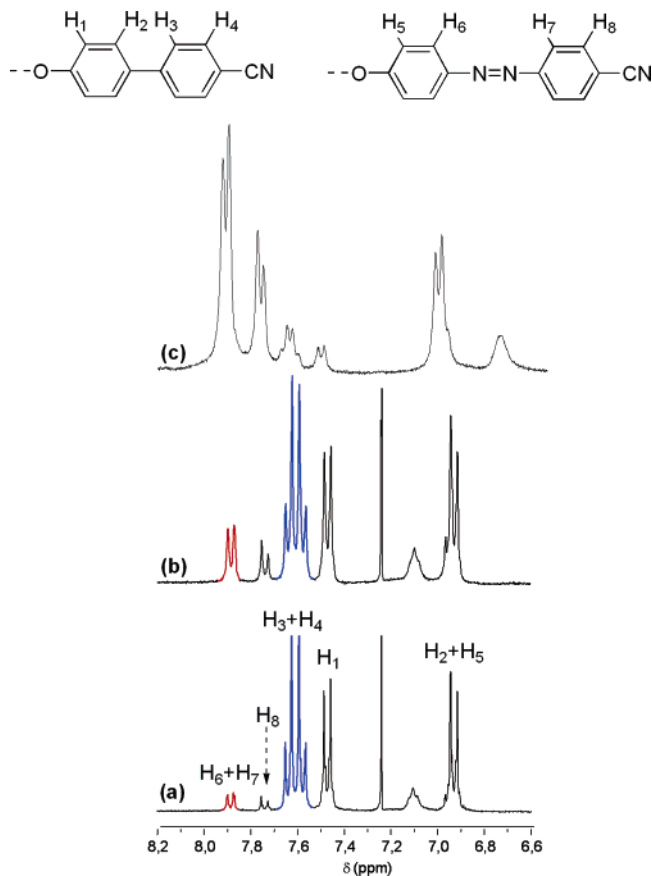


Figure 3. ¹H NMR spectra of the codendrimers corresponding to the aromatic region: (a) PPI-CNB/AZO-90/10 taken in CDCl₃ at room temperature, (b) PPI-CNB/AZO-80/20 taken in CDCl₃ at room temperature, and (c) PPI-CNB/AZO-20/80 taken in tetrachloroethane-*d*₂ at 65 °C. The resonances of the aromatic protons corresponding to each comonomer are indicated.

A conventional multi-fold chemical modification of the free amine groups by an amidation reaction was performed using an acid function previously activated by a pentafluorophenyl ester for the reaction to proceed more efficiently.^{44,46} Dendrimers were prepared by reacting a 10–15% excess of M-CNB and/or M-AZO in dichloromethane under reflux. The reaction proceeded in solution and the final product was isolated from the reaction medium by precipitation of the dendrimers with hexane—except for PPI-AZO and PPI-CNB/AZO-20/80, which precipitated during the course of the reaction. The dendrimers were isolated as air-stable solids whose solubility depended on the AZO content. For instance, the solubility in chlorinated solvents decreased as the proportion of the AZO comonomer increased. Therefore, dendrimers containing either 0%, 10%, or 20% of the AZO monomer were very soluble in chlorinated organic solvents but higher AZO contents (i.e., 80% or 100%) gave materials that are soluble in hot 1,1,2,2-tetrachloroethane but not in dichloromethane or chloroform. It is well-known that dendrimers tend to retain small molecules within the interior cavity,⁴⁷ and, for this reason, the dendrimers were thoroughly dried at 80 °C under vacuum until volatile compounds were

(46) Schenning, A.; Elissen-Roman, C.; Weener, J. W.; Baars, M.; van der Gaast, S. J.; Meijer, E. W. *J. Am. Chem. Soc.* **1998**, *120*, 8199–8208.

(47) Seebach, D.; Lapierre, J. M.; Skobridis, K.; Greiveldinger, G. *Angew. Chem., Int. Ed. Engl.* **1994**, *33*, 440–442.

Table 1. Content on the AZO Co-monomer Calculated by ¹H NMR and UV-vis Spectroscopy^a

dendrimer	AZO content (molar %) ^b			molar mass and molecular composition ^c			
	theoretical	¹ H NMR	UV-Vis	mass calcd ^d	mass exp	CNB/AZO ratio ^e	relative abundance (%)
PPI-CNB				7470.4	7471.4	16/0	100
PPI-CNB/AZO-90/10	10	9	7	7526.4	7577.4	13/3	8
					7549.3	14/2	21
					7521.4	15/1	45
					7493.4	16/0	26
PPI-CNB/AZO-80/20	20	18	17	7554.5 ^c	7633.3	11/5	8
					7605.4	12/4	15
					7577.4	13/3	27
					7550.3	14/2	27
					7521.3	15/1	16
					7494.3	16/0	7
PPI-CNB/AZO-20/80	80	85	77	7834.6 ^d	7916.4	0/16	10
					7886.4	1/15	18
					7858.0	2/14	24
					7835.3	3/13	21
					7807.3	4/12	18
					7779.4	5/11	9
PPI-AZO	100		74	7918.6 ^d	7920.3	0/16	29
					7530.0	0/15	16
					7139.8	0/14	21
					6750.6	0/13	17
					6364.4	0/12	17

^a Molar mass and molecular composition of the dendrimers determined by MALDI-TOF mass spectrometry. ^b Average AZO content per dendritic mole given as a molar percentage. ^c MALDI-TOF conditions for PPI-CNB: matrix, dithranol; solvent, dichloromethane; parent peak corresponding to the protonated species [M + H]⁺. For PPI-CNB/AZO-90/10 and PPI-CNB/AZO-80/20: matrix, α -cyano-4-hydroxycinnamic acid/sodium iodide (1:1); solvent, dichloromethane; peaks corresponding to [M + Na]⁺ ionic species. For PPI-CNB/AZO-20/80 and PPI-AZO: matrix, dithranol; solvent, dichloromethane/TFA (20:1); peaks corresponding to the protonated species [M + H]⁺. ^d Calculated molar mass. In the case of condendrimers the value was calculated for a given CNB/AZO ratio in relation to the 16 free amino groups at the periphery of the unmodified dendrimer: 14:2 for PPI-CNB/AZO-90/10; 13:3 for PPI-CNB/AZO-80/20; 3:13 for PPI-CNB/AZO-20/80. ^e CNB/AZO ratio given in relation to the 16 free amino groups at the periphery of the unmodified dendrimer.

not detected at low temperatures by thermogravimetric analysis (TGA).

A combination of analytical techniques was used to gain full structural information on the dendrimers together with verification of their purity, namely, elemental analysis; UV-vis, IR, ¹H, and ¹³C NMR spectroscopy; GPC; and MALDI-TOF spectrometry.

¹H NMR and UV-vis spectroscopy proved to be useful in estimating the average composition of the dendrimers. Distinct proton resonances were observed between 6.8 and 8.0 ppm in the corresponding ¹H NMR spectra, and these are associated with each functional unit (see Figure 3). Comparison of the integrations of the appropriate ¹H NMR signals made it possible to determine the average relative concentration of each comonomer in a given codendrimer. The values obtained are collected in Table 1 and are in fair agreement with theoretical values, thus confirming the similar reactivity of the two comonomers in the condensation reaction.

UV-vis characterization of samples in 1,1,2,2-tetrachloroethane was also used to evaluate the average content of azobenzene units within the dendritic molecule. The spectra of the AZO/CNB codendrimers are identical, within experimental error, to the sum of the spectra of the two separate monomers, M-AZO and M-CNB (see Figure 4). The spectra show two intense bands at 298 and 368 nm corresponding to the $\pi\pi^*$ transition of the cyanobiphenyl and *E*-azobenzene units, respectively. In addition, a weak band is observed at 460 nm corresponding to the symmetry forbidden $n\pi^*$ transition of the *E*-azobenzene unit. The fact that the λ_{\max} values of the bands do not vary significantly when compared to those of the monomers indicates that the functional units

attached to the dendrimer exterior behave independently in solution. As described for other dendrimers containing azobenzene units at the periphery, in the absence of mutual interactions, the intensity of $\pi\pi^*$ band corresponding to the *E*-azobenzene unit would vary with the number of azobenzene groups in an additive way according to the Beer-Lambert law.^{48,49} Therefore, the AZO content of the dendrimers was estimated by establishing a correlation between the absorbance at 368 nm of the M-AZO at different concentrations and that of the codendrimers. The values found are collected in Table 1 and are closely related to the theoretical ones. However, if the same estimation is carried out on the azo-containing homodendrimer, PPI-AZO, an abnormally low content of the azo comonomer is calculated, 74% versus the expected 100%. This deviation from the expected value can be attributed to incomplete functionalization of the free amino groups at the PPI-(NH₂)₁₆ dendrimer periphery.

MALDI-TOF mass spectrometry was used to ascertain the extent of substitution at the periphery. Results and experimental conditions are collected in Table 1. Dendrimer PPI-CNB showed only the parent peak ([M + H]⁺) at 7471.4, indicating that all 16 amine end groups had been modified. In contrast, several species were observed in the MALDI-TOF spectrum of PPI-AZO and these are attributed to incomplete coupling of the PPI-(NH₂)₁₆ dendrimer (see Figure 5a). The parent peak at 7920.3, corresponding to the fully functionalized dendrimer ([M + H]⁺) with 16 azoben-

(48) Nithyanandhan, J.; Jayaraman, N.; Davis, R.; Das, S. *Chem. Eur. J.* **2004**, *10*, 689–698.

(49) Cheon, K. S.; Kazmaier, P. M.; Keum, S. R.; Park, K. T.; Buncel, E. *Can. J. Chem.* **2004**, *82*, 551–566.

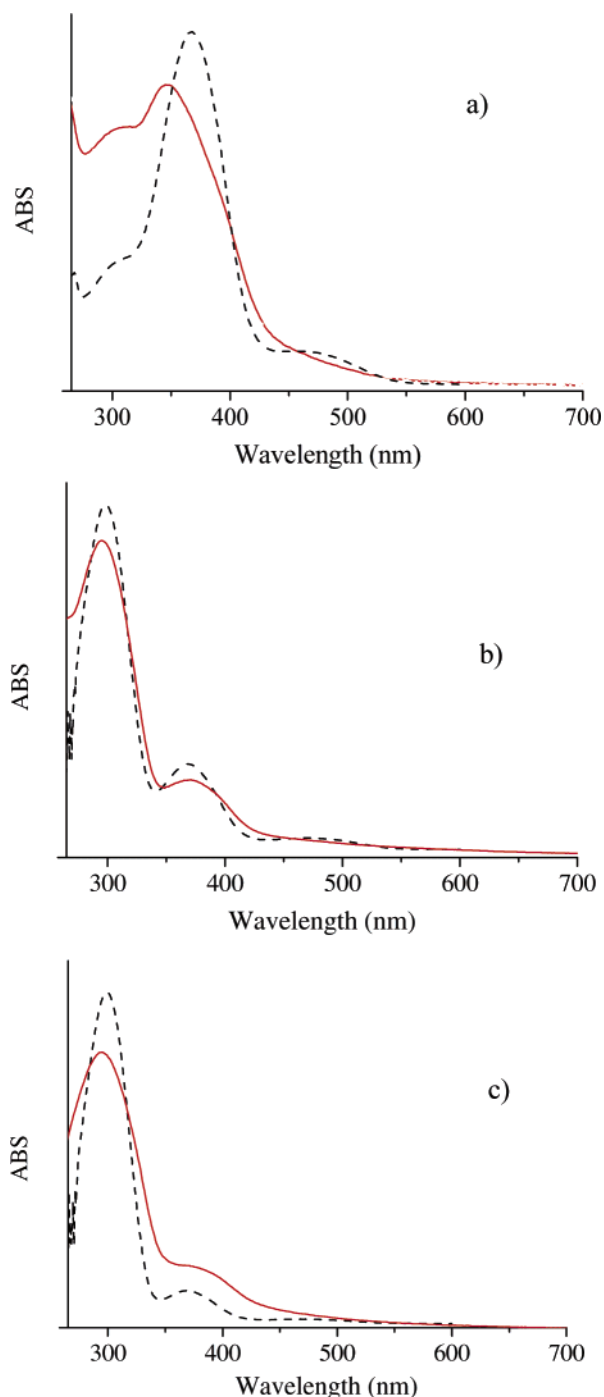


Figure 4. Absorption spectra of tetrachloroethane solutions (dashed line) and films (continuous line) of PPI-CNB/AZO dendrimers: (a) 20/80, (b) 80/20, (c) 90/10.

zene terminal groups, was observed along with peaks corresponding to dendrimers missing several azobenzene groups (from 1 to 4). Assuming that all the species have the same response to the mass detector, we can assess the relative amounts of the different species from the relative intensities of the peaks.⁴⁵ On this basis, about 29% of the material corresponds to the fully functionalized dendrimer (PPI-(AZO)₁₆). We relate the presence of imperfect structures to the aforementioned limited solubility of the AZO-containing dendrimers in common solvents. The sequential incorporation of 4-cyanoazobenzene units progressively decreases the solubility of the reacting dendrimer, causing precipitation from the reaction medium, dichloromethane, and limiting the

entire modification of the PPI-(NH₂)₁₆ dendrimer periphery. The incorporation of 4-cyanobiphenyl units improves the solubility; therefore, defective structures due to incomplete coupling were not detected by MALDI-TOF analysis of the different codendrimers in these cases.

MALDI-TOF mass spectra of the codendrimers showed several main peaks corresponding to proton or sodium ionized molecular ions depending on the matrix (see Table 1). The assignment of the peaks was made by considering the possible structures expected for a random modification of the periphery of PPI-(NH₂)₁₆. As an example, the mass spectrum of PPI-CNB/AZO-80/20 is presented in Figure 5b. From a statistical point of view, the chemical modification of PPI-(NH₂)₁₆ with a mixture of M-CNB and M-AZO in an 80:20 molar ratio should give mixtures of functionalized dendrimers that have different composition but consist mainly of dendritic molecules having thirteen 4-cyanobiphenyl units and three 4-cyanoazobenzene units, PPI-(CNB)₁₃(AZO)₃ (theoretical mass of 7554.5). Correlation of the calculated weights of the possible structures with the peaks observed in the spectrum and their relative intensities indicates that PPI-CNB/AZO-80/20 essentially contained 27% of PPI-(CNB)₁₃(AZO)₃ and 27% of PPI-(CNB)₁₄(AZO)₂, together with minor amounts of other dendrimeric compositions. Similarly, PPI-CNB/AZO-20/80 mainly consisted of 24% of PPI-(CNB)₂(AZO)₁₄ and 21% of PPI-(CNB)₃(AZO)₁₃. PPI-CNB/AZO-90/10 consisted of 45% PPI-(CNB)₁₅(AZO)₁, 26% of PPI-(CNB)₁₆(AZO)₀, and 21% of PPI-(CNB)₁₄(AZO)₂.

Thermal Characterization of the Materials. The thermal stability of the dendrimers was evaluated by TGA under a nitrogen atmosphere and showed a clear correlation with the azobenzene content. The results are presented in Table 2 and Figure 6. There are very few reports on the thermal stability of azobenzene dendrimers, although it has been reported that the thermal stability of PAMAM dendrimers increases on functionalization with an azo moiety.⁴⁹ The non-functionalized PPI-(NH₂)₁₆ showed good thermal stability—as deduced from the TGA curve, which showed a 5% weight loss temperature of 370 °C and 10% of 381 °C. Similar behavior was determined for PPI-CNB. In contrast, PPI-AZO was found to have only a moderate thermal stability. The TGA curve showed that degradation took place in several steps, with 5% weight loss at 208 °C. In the same way, comparison of the different codendrimers revealed that the thermal stability decreases as the content of 4-cyanoazobenzene increases.

The phase behavior of the dendrimers was investigated by DSC and POM in combination with X-ray diffraction. Transition temperatures and thermodynamic parameters are summarized in Table 2. All the dendrimers were found to be liquid crystalline. Upon heating, the dendrimers melted to give an anisotropic melt identified by polarizing optical microscopy to be SmA from the fan-shaped texture coexisting with a homeotropic texture. The lamellar nature of the mesophase was confirmed by X-ray diffraction. As an example, from the PPI-CNB/AZO-80/20 diffraction pattern, the distance between layers calculated from the diameter of the first-order Bragg peak was 41.6 Å, which is consistent

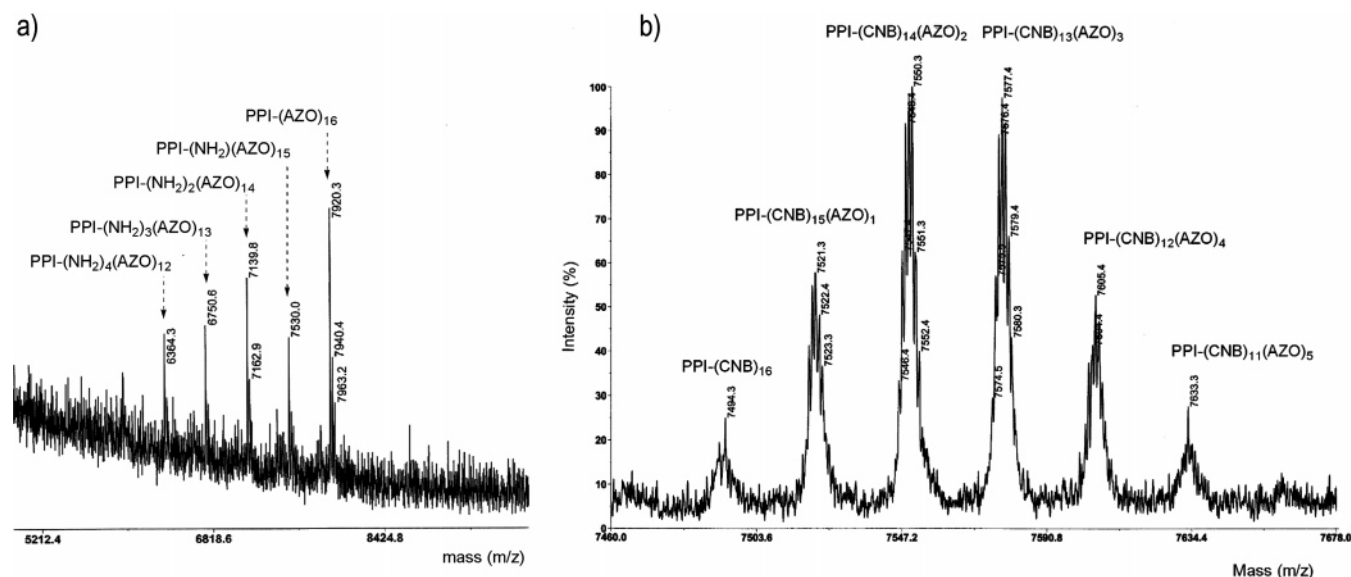


Figure 5. MALDI-TOF mass spectra and peak assignments: (a) PPI-AZO, (b) PPI-CNB/AZO-80/20.

Table 2. Thermal Stability, Phase Transitions, and Thermodynamic Data for the Dendrimers

dendrimer	TGA analysis ^a		DSC analysis ^b			mesophase
	5% wt loss	10% wt loss	T_g	T_m (ΔH)	T_i (ΔH)	
PPI-CNB	338	358	<i>c</i>	104 (275)	125 (69)	SmA
PPI-CNB/AZO-90/10	330	354	<i>c</i>	100 (288)	130 (70)	SmA
PPI-CNB/AZO-80/20	281	343	<i>d</i>	93 (232)	129 (67)	SmA
PPI-CNB/AZO-20/80	239	273	36 ^e	100 (96)	151 (58)	SmA
PPI-AZO	208	237	31		140 (49)	SmA

^a Temperatures at which 5% or 10% of the initial mass was lost ($^{\circ}\text{C}$). ^b Temperatures given in $^{\circ}\text{C}$. T_g , glass transition temperature; T_m , melting temperature; T_i , isotropization temperature. Transition enthalpies, ΔH , are given in kJ/mol using the average molecular weight calculated from the composition estimated by MALDI-TOF mass spectrometry. ^c Not detected. ^d T_g was not detected, but a cold crystallization was observed in the DSC curve. ^e Cold crystallization phenomena above T_g .

with a parallel conformation of the dendrimer in the layers.⁵⁰

In agreement with the literature results, PPI-CNB showed a SmA phase between 104 and 125 $^{\circ}\text{C}$.⁴⁴ According to the DSC curves, the dendrimer crystallized on cooling, and the T_g was not detected. In contrast, PPI-AZO was isolated from the reaction as a semicrystalline solid that melted at 123 $^{\circ}\text{C}$ to give the mesophase before the transition to the isotropic state at 141 $^{\circ}\text{C}$. Upon cooling this sample did not crystallize but solidified to form a supercooled transparent glassy film. The DSC scan corresponding to the second heating cycle showed a T_g at 31 $^{\circ}\text{C}$ and a broad SmA-isotropic liquid transition at 140 $^{\circ}\text{C}$. However, the sample crystallized on standing at room temperature for over 2 weeks, as evidenced by new DSC scans in which different melting peaks were observed.

As one would expect, codendrimers showed thermal behavior halfway between the homodendrimers. On cooling from the isotropic liquid state, PPI-CNB/AZO-20/80 formed a mesomorphic glass, but the heating DSC scan of this glass revealed a cold crystallization process above the T_g (36 $^{\circ}\text{C}$) and melting of the crystalline fraction at 100 $^{\circ}\text{C}$. On increasing the CNB content the tendency to crystallization also increased. It was deduced from the DSC curves that on cooling, crystallization of PPI-CNB/AZO-80/20 is slow but there is also a cold crystallization process on heating the

supercooled glass, and the T_g could not be calculated accurately. In the case of PPI-CNB/AZO-90/10 crystallization occurs on cooling the mesomorphic melt.

Dichroism and Birefringence of Films. One of the goals of the present work was to evaluate the photo-induced optical anisotropy in PPI-CNB/AZO films under different irradiation conditions. In order to obtain standardized samples, all of the films investigated were quenched from the isotropic phase to RT, and the optical absorption was then measured in order to assess their initial state. On repeating the quenching processes from temperatures about 20 $^{\circ}\text{C}$ above the T_i , PPI-AZO films showed a progressive and rather fast degradation; consequently, in this case it was not possible to complete the optical study under the same conditions as for the rest of compounds.

The absorption spectra of PPI-CNB/AZO-20/80, 80/20 and -90/10 thin films are shown in Figure 4. In spectra 4b and 4c, corresponding to the codendrimer films with lower azo contents, it is possible to identify the same bands as obtained in solution, albeit significantly broader. In the spectrum of the PPI-CNB/AZO-20/80 film, the $\pi\pi^*$ transition band at $\lambda_{\text{max}} \approx 350$ nm is broader but also blue-shifted by ≈ 20 nm as compared to the equivalent band in solution. This shift is usually attributed to the presence of H-type azobenzene aggregates in side-chain polymers, and it has also been reported in dendrimer films.^{41,42}

As mentioned in the introduction, photo-orientation of azo dendrimer films has not been widely investigated. Although

(50) Donnio, B.; Barbera, J.; Gimenez, R.; Guillon, D.; Marcos, M.; Serrano, J. L. *Macromolecules* **2002**, *35*, 370–381.

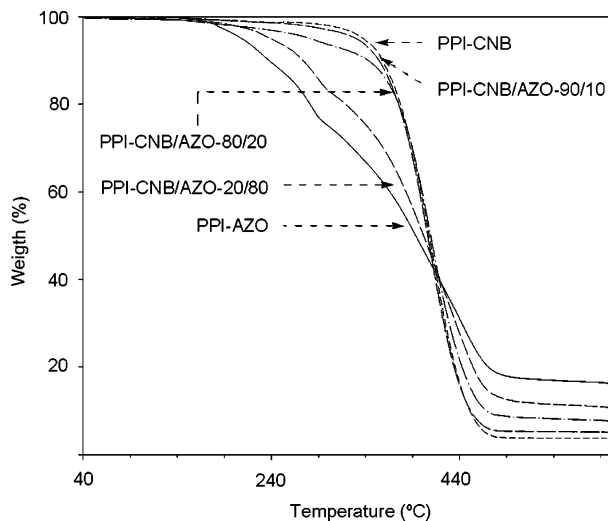


Figure 6. Weight loss curves of the investigated dendrimers at 10 °C/min under a nitrogen atmosphere.

important differences in the photo-orientational behavior of dendrimers thin films have been described, the induction of a stable orientation after polarized UV or blue irradiation has not been reported. The purpose of the work described here was to investigate the capability of photo-addressable PPI dendrimers with cyanoazobenzene substituents to achieve a stable macroscopic alignment at RT. In order to study the photo-orientation process, quenched films from the isotropic phase were irradiated at 25 °C with vertically polarized 488 nm light (60 mW/cm²). The polarized optical absorption spectra of the irradiated films were measured at RT with linearly polarized light (vertical/horizontal). Linear dichroism due to a preferential alignment of *E*-azobenzene molecules in a plane perpendicular to the polarization direction of the light was induced in the three codendrimers. Dichroism values about $D = 0.2$ were measured in PPI-CNB/AZO-20/80 films after blue irradiation for 25 min. Although it was found that this dichroism tended to decrease for some time after irradiation was ceased, it achieved an ultimate stable value. In Figure 7a, the polarized absorption spectra of PPI-CNB/AZO-20/80 measured 20 h after irradiation are shown. Somehow lower D values have been reported for carbosilane dendrimers with propoxyazobenzene groups that decreased to zero after several hours at RT.⁴³ The higher viscosity expected at RT for our PPI codendrimer as compared with the first generation carbosilane could explain this different behavior. In the linear dichroic spectra, the decrease in the absorption of vertical light (parallel to the polarization of the blue light) was markedly higher than the increase of the absorption of horizontal light (perpendicular). More prolonged irradiation gave rise to higher dichroism ($D > 0.3$) and both parallel and perpendicular absorptions lower than that for the non-irradiated film. If the orientation of the azo chromophores under blue irradiation took place with the same probability in all directions in the plane perpendicular to the polarization of the 488 nm light, the decrease would be twice as large as the increase. Thus, these results suggest that the orientation of the azo chromophores tends to be homeotropic in these films. This tendency toward homeotropic alignment was also a characteristic observed when studying samples under polarizing optical microscopy.

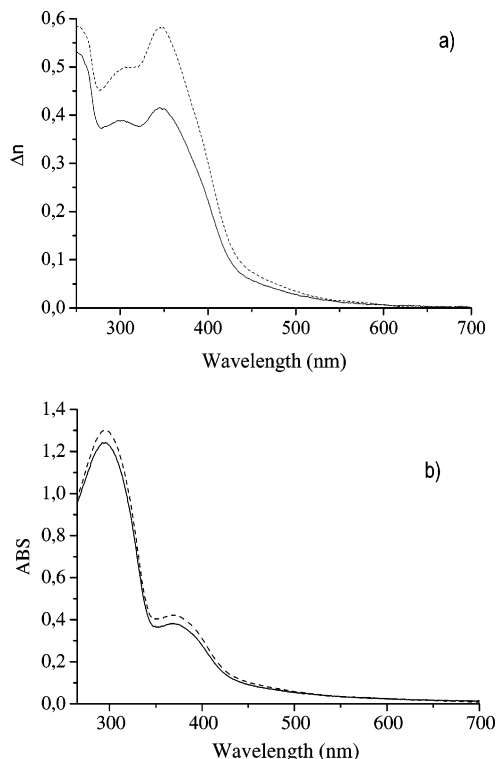


Figure 7. Polarized absorption spectra, horizontal (dashed line) and vertical (continuous line), of PPI-CNB/AZO dendrimer films taken 20 h after irradiation for 1500 s with 488 nm vertical light. (a) 20/80, (b) 80/20.

In the case of PPI-CNB/AZO-80/20 and -90/10 films, under the same experimental conditions, a lower but still evident dichroism was measured in the absorption band of azo substituents as well as in the biphenyl group band, as shown in Figure 7b for the 80/20 dendrimer. The interaction between photo-active azobenzene and photo-inactive units and the subsequent orientation of the latter moieties has already been reported in a number of papers concerning side-chain azo copolymers.^{15,20,21,51}

With regard to birefringence (Δn) measurements, we studied the photo-induction of Δn upon irradiation with linearly polarized 488 nm light (60 mW/cm²) at 25 °C in films quenched from the isotropic phase. The optical density of the films at 488 nm was lower than 0.05 so we did not take into account the attenuation of the 488 nm exciting light when the results of the different films were compared. The evolution with time of Δn is shown in Figure 8. As expected, the birefringence increased with the azo content due to the photo-induced orientation of *E*-azobenzene molecules. However, an irradiation time of 1500 s was not sufficient to reach a saturation value. In fact, under the experimental conditions outlined above, Δn increased for a few hours and reached saturation values higher than 0.04 for PPI-CNB/AZO-20/80 and slightly lower than 0.008 and 0.005 for PPI-CNB/AZO-80/20 and -90/10, respectively. In agreement with the linear dichroism results, when the 488 nm light was switched off a decrease in Δn was observed in all the samples, and this can be associated with the back thermal relaxation of *Z* molecules to the *E* state. One day after the prolonged irradiation, a stable Δn value of about 0.035 was measured

(51) Rodriguez, F. J.; Sanchez, C.; Villacampa, B.; Alcalá, R.; Cases, R.; Millaruelo, M.; Oriol, L. *Polymer* **2004**, *45*, 2341–2348.

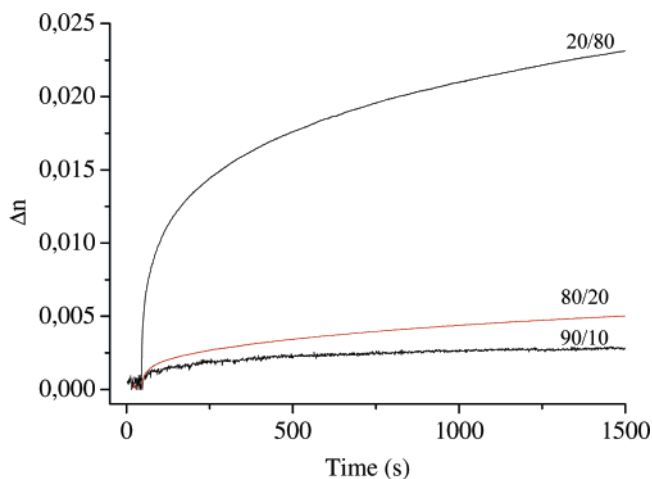


Figure 8. Evolution of the birefringence with time in PPI-CNB/AZO dendrimer films under irradiation at RT with 488 nm linearly polarized light.

for the PPI-CNB/AZO-20/80 codendrimer whereas $\Delta n \approx 0.005$ was obtained for the 80/20 codendrimer films.

Part of the practical interest in dendrimers comes from the expected rapid optical response; however, the photoanisotropy induction rate was rather slow in the films under study. It has been reported in a number of papers concerning side-chain polymers that both the kinetics and saturation values of photo-induced birefringence under 488 nm light may be very different if the films are previously irradiated with UV light.^{29–31,52} However, there are a few references in which the effect of UV pre-irradiation on the photo-orientation properties of thin dendrimer films has been analyzed. An increase in the induction rate, along with similar saturation values for the order parameter have been reported for carbosilane dendrimers.⁴³ In order to assess the influence of UV pre-irradiation, films of PPI-CNB/AZO-20/80 and -80/20 were irradiated for different time intervals with unpolarised light from a Hg pressure lamp (0.5 mW/cm^2). The optical absorption spectra measured a few minutes and 20 h after irradiation for 5 min with unpolarized UV light are shown in Figure 9. Irradiation leads to a decrease in the $\pi\pi^*$ band absorbance of the *E* moieties as compared to the quenched films, while the band due to the presence of *Z* isomers at about 450 nm is clearly visible. Besides, despite the fact that the bands of CNB and AZO moieties are overlapped, a shift of the azo $\pi\pi^*$ band to longer wavelength can be observed in PPI-CNB/AZO-20/80 films. The spectra taken 20 h after irradiation are similar to the initial ones, where the *Z* isomer absorption is not appreciable and the *E* isomer absorption has been practically recovered. The time evolution of the birefringence of UV pre-irradiated films under polarized blue light irradiation is shown in Figure 9c for PPI-CNB/AZO-20/80. It can be seen that although the qualitative evolution is similar both with and without pre-irradiation, birefringence increases faster and values achieved upon prolonged irradiation are also higher ($\Delta n \approx 0.045$ is reached upon irradiation for several hours) in pre-irradiated films as compared with thermally quenched ones. In the case

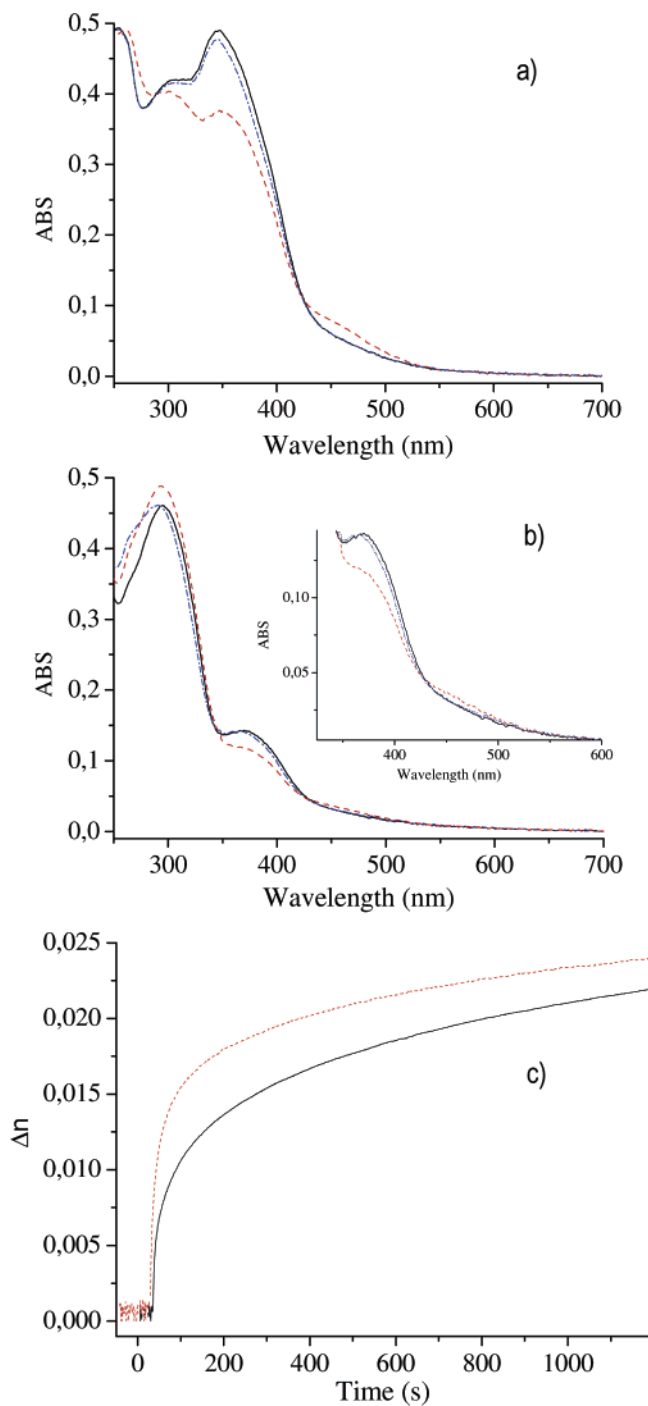


Figure 9. Absorption spectra of PPI-CNB/AZO-20/80 (a) and 80/20 (b) films measured after 5 min irradiation with depolarized UV light. The dashed lines correspond to spectra taken 2 min after the irradiations were performed, and the dot-dashed spectra were measured 20 h after the irradiation. (c) Birefringence of PPI-CNB/AZO-20/80 measured at RT under 488 nm linearly polarized light after quenching from the isotropic phase to RT (continuous line) and after pre-irradiation with depolarized 350 nm light (dashed line).

of PPI-CNB/AZO-80/20 films, the results were qualitatively similar and higher values of Δn are reached after UV irradiation, but the differences were less significant. There are several effects that can be taken into account to explain these results. First, it was reported that the concentration of *Z* isomers after UV irradiation causes the decrease in the T_i of side chain azopolymers.²⁷ Furthermore, it is well-known that azo aggregates, which can hinder the orientation processes, are broken upon UV irradiation, both in polymer^{29–31,52}

(52) Rodríguez, F. J.; Sanchez, C.; Villacampa, B.; Alcalá, R.; Cases, R.; Collados, M. V.; Hvilsted, S.; Strange, M. *Polymer* **2004**, *45*, 6003–6012.

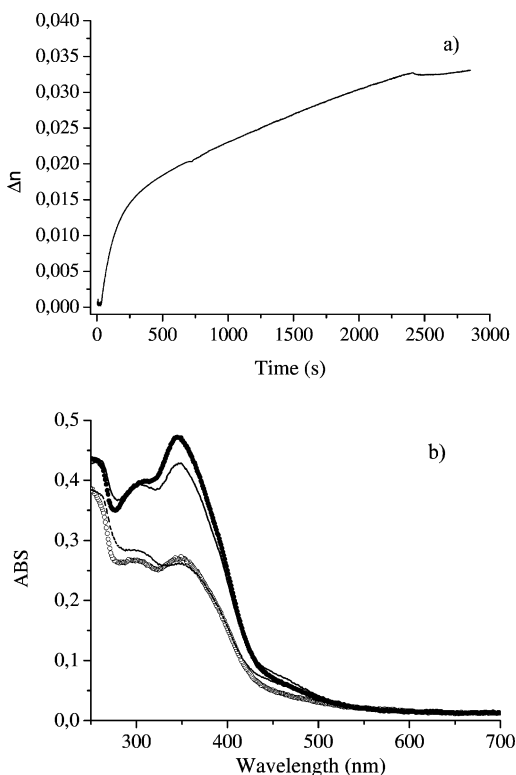


Figure 10. (a) Evolution of birefringence with time in PPI-CNB/AZO-20/80 dendrimer film under irradiation at RT with 350 nm linearly polarized light. (b) Polarized absorption spectra of PPI-CNB/AZO-20/80 dendrimer film taken a few minutes (horizontal, continuous line; vertical, dashed line) and 20 h (horizontal, ●; vertical, ○) after irradiation for 2400 s with 350 nm vertical light.

and dendrimer thin films.^{42,43} As mentioned above, the absorption spectra of the dendrimer films taken a few minutes after UV irradiation show the presence of *Z* isomers whereas the red shift of the *E* isomer absorption suggests that the breakdown of H aggregates takes place upon UV irradiation. Both effects can contribute to the increase in azo mobility in pre-irradiated films and could account for the different time evolution shown in Figure 9c. As far as PPI-CNB/AZO-80/20 films are concerned, a lower level of aggregation of the azo chromophores could explain the smaller difference between the evolution of Δn with and without UV pre-irradiation.

To complete the study, linear dichroism and birefringence were also measured for PPI-CNB/AZO-20/80 films irradiated with UV polarized light. As shown in Figure 10a, the time evolution of birefringence measured in films quenched from the isotropic phase was similar to that obtained under blue irradiation. When the UV irradiation was switched off, an initial small decrease in the birefringence was observed followed by a slight increase before a saturation value was finally achieved. This behavior is consistent with the optical dichroism results. The polarized absorption spectra measured immediately after the data shown in Figure 10a were recorded are shown in Figure 10b along with those measured 1 day later. It should be noted that after 1 day, the *Z* absorption band is not visible in either vertical or horizontal spectra whereas both *E* absorptions at about 350 nm have increased, with the dichroic ratio being slightly higher. This fact implies that, in the back *Z*-to-*E* isomerization process, *Z* isomers are preferentially oriented following the photo-

induced direction. This photo-orientational behavior is completely different to that observed in carbosilane dendrimer films under polarized UV irradiation.^{42,43} In some of these dendrimers, an increase in the order parameter was observed at the beginning, but under prolonged irradiation (with 5.3 mW/cm²) it decreased almost to zero. This behavior was connected with the increase in the *Z* isomer content during UV irradiation and the subsequent degeneration of the orientational order due to its low anisometry.⁴² Thus, the concentration of *Z* isomers, which depends among other parameters on the UV light intensity, is expected to play a fundamental role in this process. In fact, a dramatic dependence of the degree of orientation on the UV irradiation dose has already been reported for side-chain azo polymers.⁵³ In the present study the intensity used was quite low and, consequently, so it should be the induced concentration of *Z* isomer in PPI-CNB/AZO-20/80 films allowing the development of stable photo-induced order with UV polarized light.

Conclusions

A series of PPI dendrimers with different numbers (up to 16) of 4-cyanoazobenzene and 4-cyanobiphenyl units randomly distributed at the periphery were prepared. The materials were characterized by different techniques but detailed information about the degree of functionalization of the terminal groups and the chemical composition was gained by MALDI-TOF spectrometry. The photo-orientation processes of films of PPI-CNB/AZO codendrimers have been studied and stable values of dichroism and birefringence under polarized blue or UV light at RT have been measured up to 24 h after irradiation.

From these results, it can be concluded that high azobenzene contents at the periphery of the dendritic molecule are required to obtain light-oriented films with a pronounced dichroism and birefringence values up to 0.045. At the same time, there are several properties that are critical to obtain good quality transparent films and these had to be adjusted by controlling the azobenzene content. Solubility and thermal stability are adversely affected by large azobenzene contents but crystallinity is lower, as in the corresponding homodendrimer PPI-AZO. A compromise between all these requirements has been reached by incorporating 20% of a photo-inactive liquid crystalline unit at the surface of the PPI dendrimer.

For PPI-CNB/AZO-20/80 films, a moderate but stable orientation has been induced by irradiation using 488 nm polarized light, with the azobenzene units disposed perpendicular to the electric field of the incident light. The observed photo-induction rate is quite slow, probably due to the formation of azobenzene aggregates that make the photo-orientational process difficult. Nevertheless, this drawback can be overcome because the kinetics of photo-induced birefringence with 488 nm light are somewhat faster if films are pre-irradiated with unpolarized UV light. It is also possible to induce a stable orientation just by irradiation with UV-polarized light.

In summary, we have demonstrated that azobenzene-containing PPI dendrimers are promising materials for the preparation of stable photo-orientable films. Work is in progress to produce dendrimers with improved solubility while maintaining a high number of azobenzene units in the dendritic molecule and a lower tendency toward homeotropic alignment.

Acknowledgment. This work was supported by the CICYT-FEDER Spanish projects MAT2003-07806-C02-01, MAT2005-06373-C02, the “Ramón y Cajal” program (MCYTMEC), and funding from the Government of Aragon. We are also grateful to the Servicio Central de Análisis, Sidi, of the Universidad Autónoma de Madrid for the MALDI-TOF analysis.

CM061727A